Janet Tate
4/97

Analysis of $YBa_2Cu_3O_7$ Films by X-ray Diffraction

by

Brandon B. Van Leer

A THESIS
submitted to
the Physics Department of
Oregon State University

in partial fulfillment of
the requirement for the
degree of

Bachelor of Science

Date

AN ABSTRACT OF THE THESIS OF

Brandon B. Van Leer for the degree of *Bachelor of Science* in *Physics*. Title: *Analysis of $YBa_2Cu_3O_7$ Films by X-ray Diffraction.*

Analysis of fully oxygenated $YBa_2Cu_3O_7$ film grown on a sapphire (Al_2O_3) substrate with a ceria (CeO_2) buffer layer by x-ray diffraction provides useful information regarding the lattice spacing, thickness of film and the strain occurring in the thin films. Particular interest was paid to the inclusion of broadening effects of the spectra due to instrumental resolution. This thesis showed that removal of instrumental broadening was not a significant factor in the strain found in the films, but posed questions about the validity of the determination of the thickness of the films.

Table of Contents

	Page
INTRODUCTION	1
Thin Films	1
Characterization	1
Superconducting Thin Films	1
Substrate	2
Buffer Layer	2
X-ray Diffraction	3
History	3
Utility	3
Limitations	4
Lattice Spacing	5
Broadening	6
Data	9
Analysis	12
$Y_1Ba_2Cu_3O_7$ film	12
CeO_2 buffer layer	15
Al_2O_3 substrate	15
Conclusion	19
Bibliography	21

Thin Films

Thin films have been studied since the turn of the century. During the first half of the century, scientists mainly explored the optical characteristics and thicknesses of different thin films. With the emergence of thin films in the microelectronic industry during the second half of the century, thin-film science has exploded so that a better understanding of the intrinsic properties of thin films may be learned (Ohring, 1992). Today, thin films are used as optical coatings to create polarizers and beam splitters as well as being used to create micro-circuitry like transistors. With the increased need to understand thin films, properties such as thickness, atomic structure, and lattice parameters (i.e. strain of the crystal, spacing between atoms) have been studied thoroughly for a variety of different substances.

Since the discovery of $YBa_2Cu_3O_7$ (YBCO), a high-T_c superconductor, many scientists have studied this substance exhaustively; probably because it is the easiest to prepare in bulk and thin-film form (Ohring, 1992). Yet, there is still much to be learned. Because of the relatively low cost with which $YBa_2Cu_3O_7$ can be prepared, it is fast gaining importance in the application of microwave devices such as transmission lines, delay lines and quasi-optical band-pass filters (Prakash et al, 1992). Using x-ray diffraction as a tool for analysis, this paper will examine the lattice spacing and crystal strain of an $YBa_2Cu_3O_7$ film grown on an Al_2O_3 (sapphire) substrate with a buffer layer of ceria (CeO_2), and analyze the importance of the inherent broadening of the diffraction peaks due to the analysis instrument itself.

The sample studied here was a 200 nm YBCO film evaporated onto a sapphire substrate with a ceria buffer layer. There are several important factors that determine the

use of one particular substrate over another. Here, Al_2O_3 offers a small dielectric constant of 9.34 at 298K (Lide, 1993), chemical stability in oxygen at the elevated temperatures that are needed during deposition, and availability as crystal wafers at low cost (Maul et al, 1994). A buffer layer of CeO_2 was introduced between the Al_2O_3 substrate and $YBa_2Cu_3O_7$ film to reduce interactions between them. Aluminum interdiffusion and lattice mismatch are common problems (Maul et al, 1994). In addition to reducing film interactions, CeO_2 has an intermediate thermal expansion coefficient of $\alpha_{CeO_2} = 11.6*10^{-6}K^{-1}$ compared to Al_2O_3's $\alpha_{Al_2O_3} = 6*10^{-6}K^{-1}$ and $YBa_2Cu_3O_7$'s $\alpha_{YBCO} = 13*10^{-6}K^{-1}$ (all at room temperature), which reduces strain caused by different thermal expansion coefficients, and also has a low dielectric constant of 7.0 (Merchant et al, 1991). Figure 1 is a representation of the film growth.

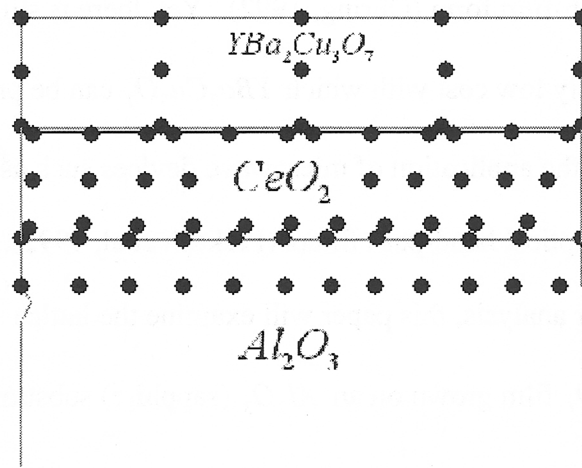

Figure 1 A representation of the set of films under analysis.

X-Ray Diffraction

In 1912, German physicist Max von Laue (1879-1960) conceived the idea of using a crystal as a three-dimensional grating since the crystal was composed of regularly spaced atoms (Hecht, 1987). He hypothesized that if x-rays were electromagnetic waves with wavelength on the order of the atomic spacing (0.1 or 0.2 nm), then they would diffract off of the crystal, thus developing x-ray diffraction. That same year, W.H. Bragg (1862-1942) and W.L. Bragg (1890-1971) studied Max von Laue's experiments intensively. W.L. Bragg mathematically characterized von Laue's experiments within a short time. With x-ray diffraction as a powerful new tool, Bragg successfully solved the structures of many crystals such as HCl, KCl, KBr and KI (Cullity, 1978). Bragg's mathematical characterization of x-ray diffraction is now known as the Bragg law- $n\lambda = 2d\sin\theta$. Experimentally, it can be used to determine the spacing between the planes of a crystal using a known wavelength and varying the angle, θ. Another way to use the Bragg Law is to use a crystal with known lattice parameters to determine an unknown wavelength.

Historically, instruments which measure x-ray spectra using a crystal of known structure are labeled x-ray spectrometers and instruments that are used to study crystalline and non-crystalline materials are named x-ray diffractometers (Cullity, 1978). Initially, these instruments were mainly used for research, but industry in microelectronics has embraced these tools as a means of failure analysis and process control. For this experimental analysis, a Siemens D5000 diffractometer operating with a $Cu\ K_{\alpha}$ line of wavelength of $\lambda = 0.15406$ nm was used.

It is useful to discuss the different scattering modes for diffraction since scattering can occur for all different types of arrangements. When atoms are arranged randomly as in gases or liquids, scattering occurs in all directions and is often weak. When atoms are arranged periodically, as in a crystal, strong scattering occurs only in a few directions, thus satisfying Bragg's law. In this manner, the amplitudes of the waves add together. Thus, strong scattering will occur when there is constructive interference of the electromagnetic waves and weak scattering will occur when there is destructive interference. While strong scattering may occur in a crystal, it will only be in certain directions. The figure below is a schematic of the diffraction of x-rays by a crystal.

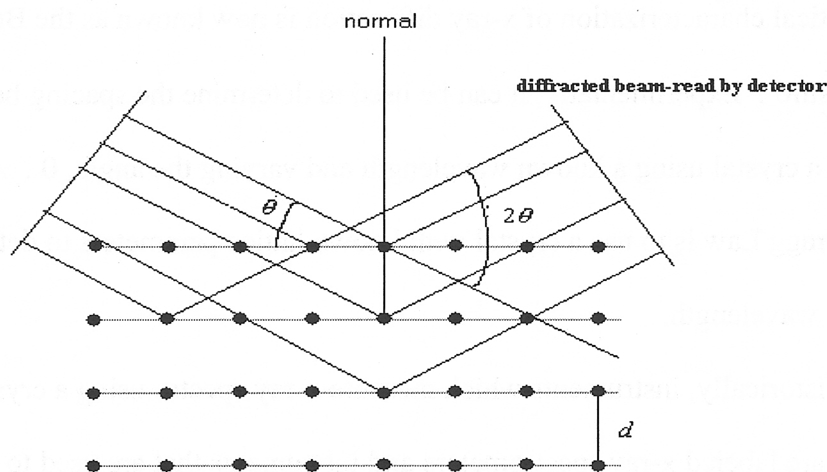

Figure 2 X-ray diffraction. Rays on the right are read up by a detector.

X-ray diffraction has therefore been used to determine the crystal structure of solids, to identify of unknown materials as well as to analyze stress and defects in crystals. Until recently, x-ray diffraction methods had not been pursued with vigor in the

study of thin-films mainly because the path length through the films was too short to produce diffracted beams of sufficient intensity (Ohring, 1992). This is due to the great penetrating power of the x-rays and is overcome by long counting times. Under these circumstances, the substrate rather than the film itself had a more detectable signal because of the strong axis orientation in the substrate. Also, the transmission electron microscope (TEM) provided the same information scanning a much smaller area of the film. X-ray diffractometers' emergence as a primary source of analysis in thin-film study is due to the nondestructive nature of the analysis as well as easy sample preparation.

An important characteristic in crystals and thin-films is the lattice spacing. It is well known that a crystal is composed of atoms that are ordered in a pattern of three dimensions. A lattice is defined as an array of points in space so arranged that each point has identical surroundings (Cullity, 1978). From this, important quantities describing the crystal such as the lattice constants in the crystal can be determined. The CeO_2 film is a cubic structure, the $YBa_2Cu_3O_7$ film is orthorhombic and the sapphire film is a hexagonal structure. The lattice constants in cubic structures are all equal to each other, while an orthorhombic structure's lattice constants are not equal though its dimensions are similar to a cubic system, $\frac{1}{d^2} = \frac{h^2}{a^2} + \frac{k^2}{b^2} + \frac{l^2}{c^2}$ where $h, k \, and \, l$ are Miller indices and d is the distance between adjacent planes (Cullity, 1978). In a hexagonal structure, the lattice constants are determined by the equation, $\frac{1}{d^2} = \frac{4}{3}\frac{h^2 + hk + k^2}{a^2} + \frac{l^2}{c^2}$. Miller indices are used to represent planes of different directions within the crystal structure.

To determine the spacing of the c-axis parameter in a film, Bragg's law was used. This law is a very powerful mathematical tool that was used extensively in this analysis. The lattice spacing is obtained from:

$$d = \frac{n\lambda}{2\sin\theta} = \frac{1*0.15406\,nm}{2*\sin\left(\frac{7.75^\circ}{2}\right)} = 0.1139 \text{ nm for the first order } YBa_2Cu_3O_7 \text{ peak}$$

located at $2\theta = 7.75^\circ$.

A more precise way of determining the spacing between the lattices is to plot d against the appropriate function of the angle. The ideal lattice spacing can be extrapolated from the plot. This is more accurate because the former method does not account for systematic errors inherent in measurement such as misalignment of the instrument, absorption in the specimen and displacement of the specimen from the diffractometer axis (Cullity, 1978). According to Cullity, no single extrapolation function can be completely satisfactory because of these systematic errors. In general, the function that gives a better straight line will show which error is largest and correction can be made from that point. In diffractometers, the strain, $\frac{\Delta d}{d}$, varies as $\cos^2\theta$ for non-cubic structures. Therefore, to eliminate the errors listed above and reduce random errors such as ordinary chance errors due to observation, extrapolating to $\frac{\cos^2\theta}{\sin\theta} = 0$ ($\theta = 90^\circ$) will be a reasonable method (Cullity, 1978).

Broadening in the x-ray diffraction peaks of the films can be caused by many factors including finite film thickness, instrumental broadening and strain. Of course, characterizing the strain in thin films as well as crystals is critical; strain needs to be

understood for many reasons. It provides insight into growing better films, details of thin-film properties, as well as defects.

Use of Bragg's law leads to a description of the strain in a thin-film. By differentiating the expression for the lattice spacing with respect to θ one obtains:

$\frac{\Delta d}{\Delta\theta} = -\frac{n\lambda\cos\theta}{2\sin^2\theta} = -\frac{n\lambda}{2}\frac{1}{\tan\theta\sin\theta}$ Dividing by $d = \frac{n\lambda}{2\sin\theta}$, one obtains

$\left|\frac{\Delta d}{d}\right| = \cot\theta\,\Delta\theta$, from which $\Delta\theta = \frac{\Delta d}{d}\tan\theta$. This relates the broadening of the peaks at full-width half-max (FWHM), $\Delta\theta$, to the strain, $\frac{\Delta d}{d}$ of the plane spacing. Plotting $\Delta\theta$ against $\tan\theta$ should yield a straight line of slope $\frac{\Delta d}{d}$ if the strain is the only factor inducing peak broadening (i.e. no instrumental broadening is observable and the thickness of the film is large).

However, both the finite thickness of the film and the instrument resolution will contribute to the broadening of the peaks. One aim of this paper is to determine whether or not these two phenomena are significant in XRD analysis. Broadening in samples due to the thickness of a film can be described by the Scherrer formula. Classically, the Scherrer formula is used to estimate the particle size of very small crystals from the broadening of the diffraction spectra (Cullity, 1978). This phenomenon is a result of incomplete destructive interference due to the finite number of scattered rays and the condition for which this occurs is the Bragg angle. If the thickness of the film was infinite, then the sum of all the scattered rays would be zero. Mathematically, it is described by $\Delta\theta_t = \frac{0.9\lambda}{t\cos\theta_B}$ and is illustrated in figure 3. Therefore, in an infinitely

thick film, $\Delta\theta_t \rightarrow 0$. The expression above can be used to estimate the inherent broadening for films of different thickness. Clearly, when the thickness is small, this type of broadening increases.

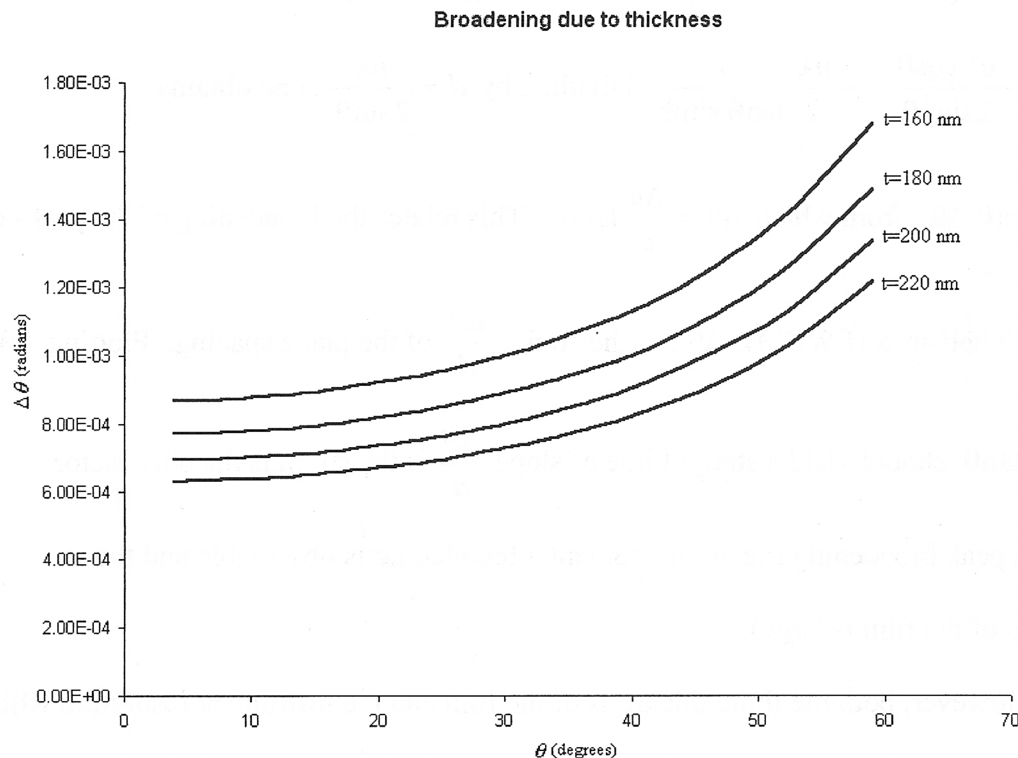

Figure 3 Broadening in films at various thicknesses. As the thickness becomes smaller, the broadening increases.

Instrumental broadening of x-ray peaks is due to many different parameters of the diffractometer such as resolution and misalignment. Using a well-annealed sample of tungsten as a standard for the subtraction of instrumental line broadening as per Warren's formula, $(\Delta\theta)^2 = (\Delta\theta)^2_{sample} - (\Delta\theta)^2_{instr.}$, the instrumental broadening can be determined (Prakash, 1992).

Data

Below, Figure 4 depicts the plot of counts versus 2θ for a YBCO film on ceria/sapphire. These counts were taken using a Siemens diffractometer with Cu radiation of wavelength, $\lambda = 1.5406\,\text{Å}$ operating at $30\,kV$. Figure 5 is a blow up of the $YBa_2Cu_3O_7$ peak for $(hkl) = (006)$ in steps of 0.02°.

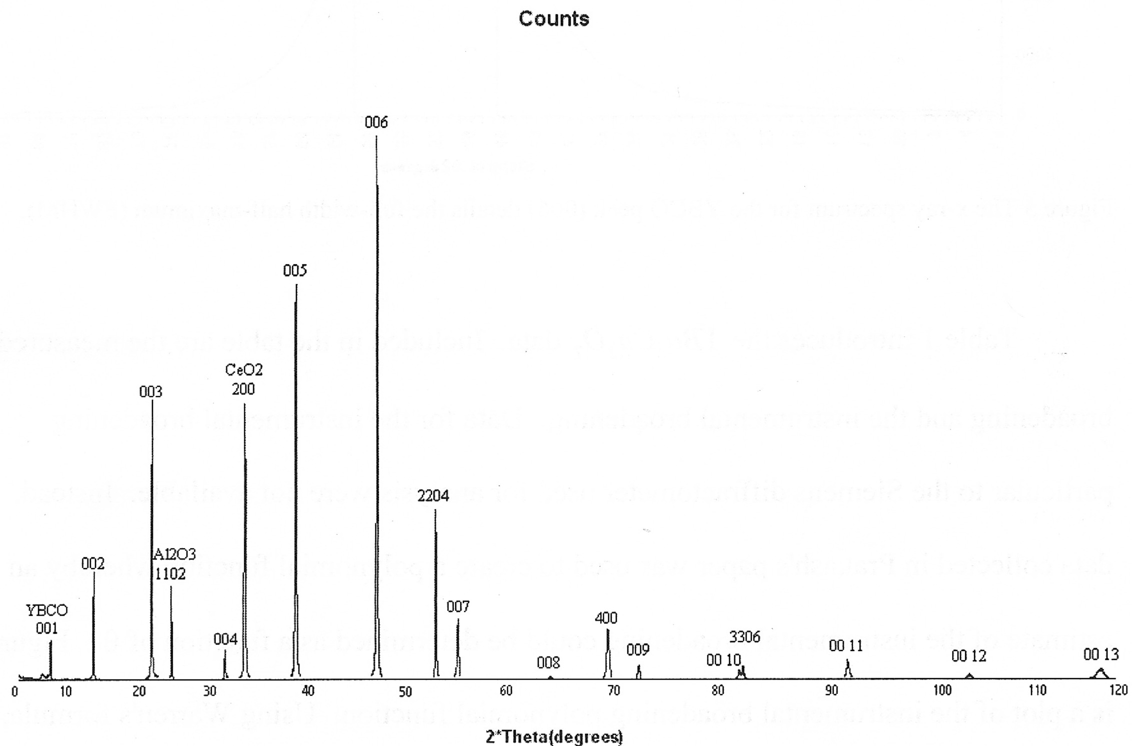

Figure 4 The x-ray spectra for the three thin films. Thirteen peaks are shown for the YBCO film, three peaks for the sapphire film and two peaks for the ceria.

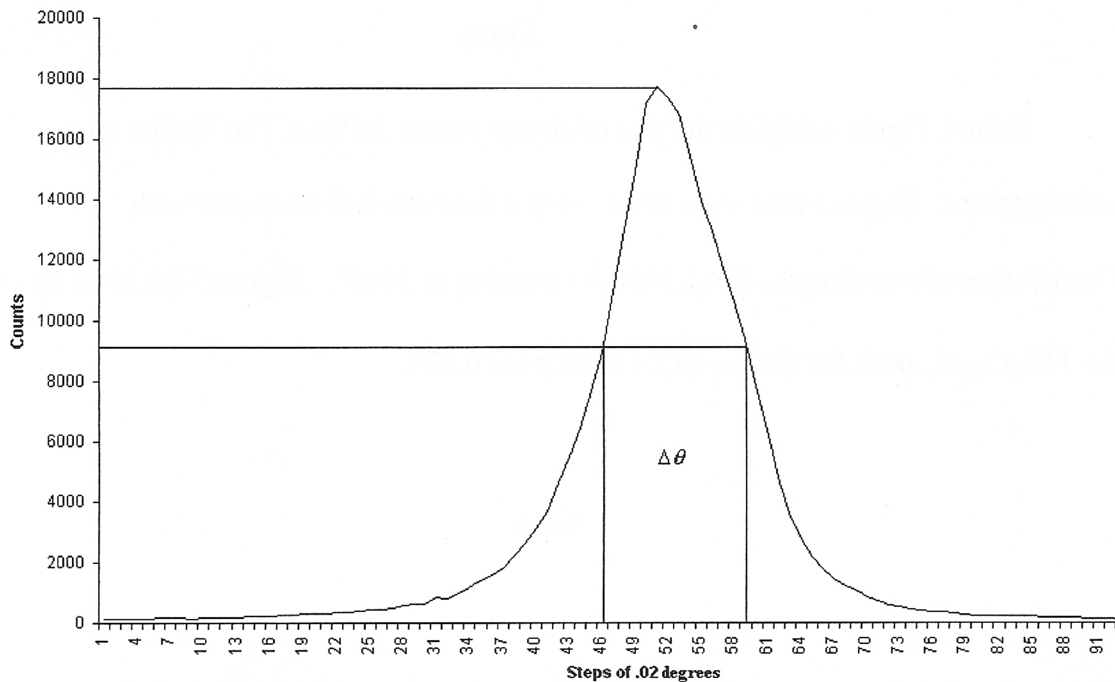

Figure 5 The x-ray spectrum for the YBCO peak (006) details the full-width half-maximum (FWHM).

Table 1 introduces the $YBa_2Cu_3O_7$ data. Included in the table are the measured broadening and the instrumental broadening. Data for the instrumental broadening particular to the Siemens diffractometer used for analysis were not available. Instead, data collected in Prakash's paper was used to create a polynomial function whereby an estimate of the instrumental broadening could be determined as a function of θ. Figure 6 is a plot of the instrumental broadening polynomial function. Using Warren's formula, the instrumental broadening was extracted, leaving peak broadening due to strain and thickness of the film.

Dangling participle

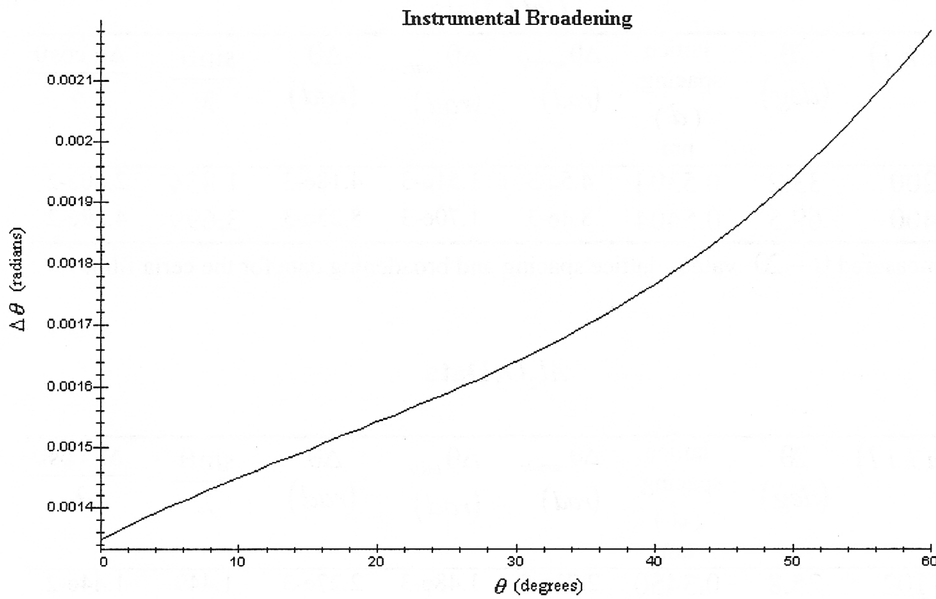

Figure 6 A plot of the function for the instrumental broadening determined from Prakash's paper.

$YBa_2Cu_3O_7$ Data

	$(h\ k\ l)$	2θ (deg)	lattice spacing (d) nm	$\Delta\theta_{sample}$ (rad)	$\Delta\theta_{instr.}$ (rad)	$\Delta\theta$ (rad)	$\frac{\sin\theta}{\lambda}$	$\frac{\Delta\theta\cos\theta}{\lambda}$
1	001	7.8	1.168	8.73E-4	9.15e-4		0.4415	
2	002	15.3	1.167	9.59E-4	9.53e-4	1.07e-4	0.8641	6.89e-4
3	003	22.8	1.166	1.03E-3	9.88e-4	8.45E-4	1.2829	6.89E-3
4	004	30.6	1.168	1.71E-3	1.02E-3	1.37E-3	1.7128	8.59E-3
5	005	38.6	1.166	2.05E-3	1.06E-3	1.75E-3	2.1454	1.07E-2
6	006	46.8	1.165	2.36E-3	1.09E-3	2.09E-3	2.5779	1.25E-2
7	007	55.0	1.168	2.53E-3	1.14E-3	2.25E-3	2.9971	1.30E-2
8	008	63.9	1.164	2.88E-3	1.19E-3	2.62E-3	3.4349	1.44E-2
9	009	73.0	1.159	3.63E-3	1.24E-3	3.41E-3	3.8610	1.59E-2
10	00 10	82.5	1.167	4.15E-3	1.31E-3	3.93E-3	4.2798	1.89E-2
11	00 11	92.2	1.155	4.79E-3	1.39E-3	4.58E-3	4.7162	2.03E-2
12	00 12	104.8	1.157	6.10E-3	1.52E-3	5.90E-3	5.1427	2.42E-2
13	00 13	118.0	1.133	1.20E-2	1.68E-3	7.41E-3	5.5636	2.54E-2

Table 1 The measured $\theta - 2\theta$ values, lattice spacing, and broadening data for the YBCO film.

CeO_2 **Data**

	$(h\ k\ l)$	2θ (deg)	lattice spacing (d) nm	$\Delta\theta_{sample}$ (rad)	$\Delta\theta_{instr.}$ (rad)	$\Delta\theta$ (rad)	$\frac{\sin\theta}{\lambda}$	$\frac{\Delta\theta\cos\theta}{\lambda}$
1	200	33.2	0.5394	4.5e-3	1.51e-3	4.18e-3	1.854	2.60e-2
2	400	69.5	0.5404	8.4e-3	1.70e-3	8.25e-3	3.699	4.39e-2

Table 2 The measured $\theta - 2\theta$ values, lattice spacing and broadening data for the ceria film.

Al_2O_3 **Data**

	$(h\ k\ i\ l)$	2θ (deg)	lattice spacing (d) nm	$\Delta\theta_{sample}$ (rad)	$\Delta\theta_{instr.}$ (rad)	$\Delta\theta$ (rad)	$\frac{\sin\theta}{\lambda}$	$\frac{\Delta\theta\cos\theta}{\lambda}$
1	$1\underline{1}02$	25.8	0.3450	2.71e-3	1.48e-3	2.27e-3	1.449	1.44e-2
2	$2\underline{2}04$	52.5	0.3483	4.5e-3	1.60e-3	4.14e-3	2.871	2.41e-2
3	$3\underline{3}06$	83.5	0.3470	6.1e-3	1.78e-3	5.83e-3	4.322	2.82e-2

Table 3 The measured $\theta - 2\theta$ values, lattice spacing and broadening data for the sapphire film.

Analysis

The lattice spacing for the $YBa_2Cu_3O_7$ film , which is the c-axis parameter above, was first calculated from each peak using Bragg's law. A mean value of $\langle d \rangle = 1.164$ nm with a standard deviation of $\sigma = .0104$ was determined. Using the extrapolation method mentioned in the X-Ray Diffraction section, which models various systematic errors, a value of $d = 1.699$ nm extrapolated. Using the method of least squares, an error of ± 0.012 nm was determined. The extrapolation is shown below in Figure 7. This extrapolation agrees with other x-ray diffractive studies on this thin film (Dumkow, 1997).

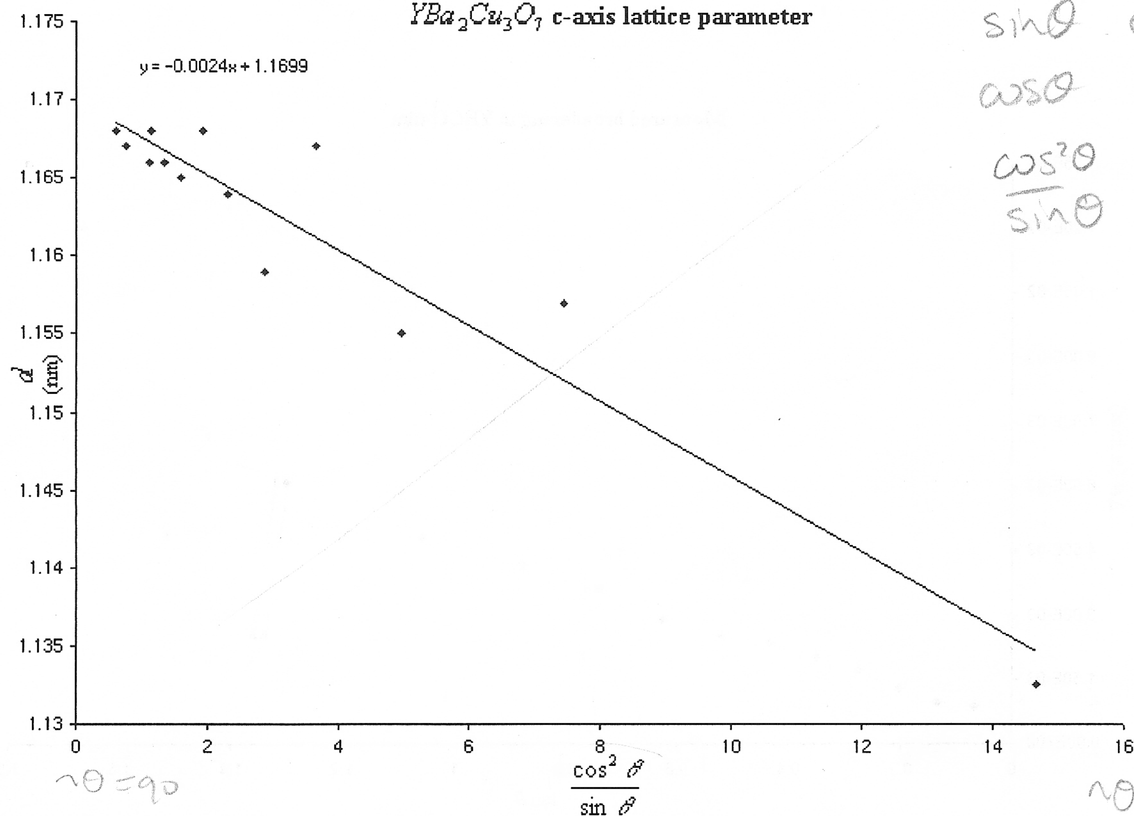

sinθ 0 → 1
cosθ 1 → 0
$\frac{\cos^2\theta}{\sin\theta}$ ∞ → 0

this is OK even tho' table 1 has wrong d this.

Figure 7 A regression plot of the c-axis parameter for the YBCO film. An extrapolated value of 1.1699 nm was determined.

The two different analyses do give different values. The mean value of the

para… …sly

such…

extr…

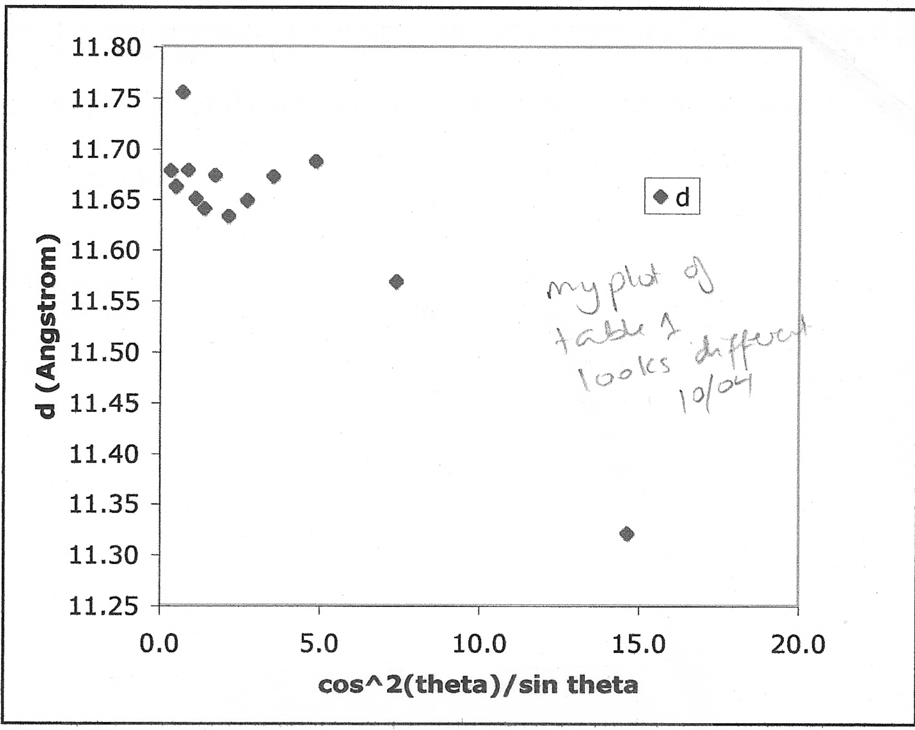

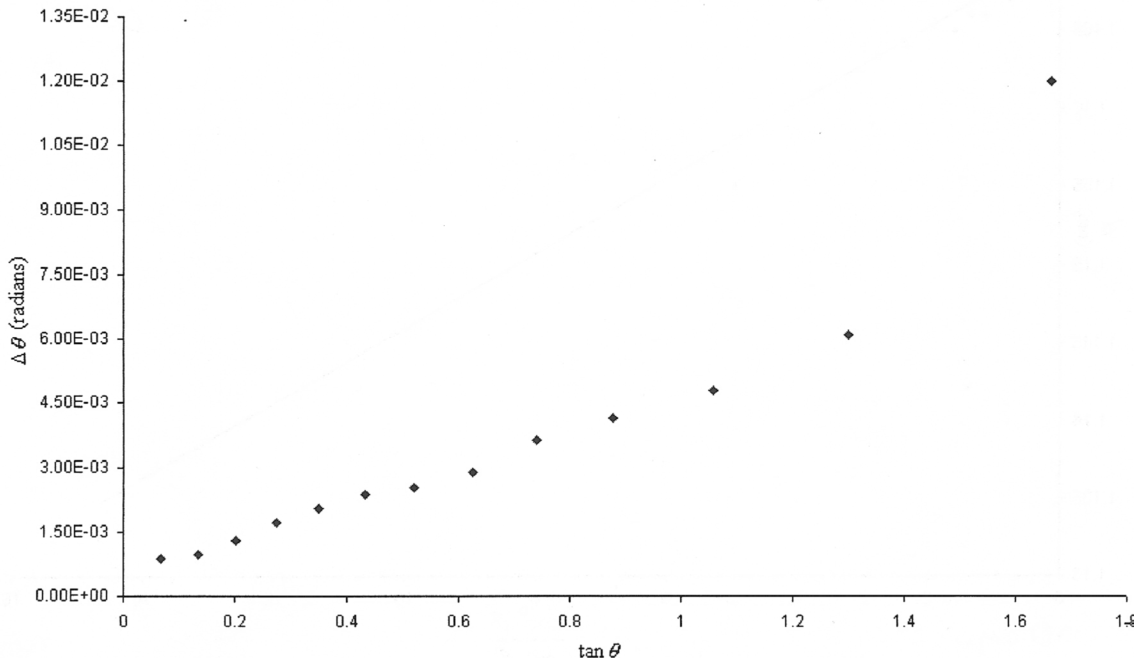

Figure 8 A plot of the measured broadening, $\Delta\theta$, vs. the tangent of the corresponding $\theta - 2\theta$ value.

By first plotting the measured broadening, $\Delta\theta$, against $\tan\theta$, the strain in the $YBa_2Cu_3O_7$ film is 0.4%, depicted above in Figure 8. The non-zero intercept is a result of finite thickness and instrumental broadening. Utilizing Warren's formula to minimize the instrumental broadening effects, the relative broadening will consist of two independent parts - one due to the actual strain in the film and one due to the thickness.

dangling participle — "the rel. broadening" does not use Warren's formula.

$\Delta\theta = \Delta\theta_{strain} + \Delta\theta_{thick}$. One therefore obtains:

$\Delta\theta = \left|\frac{\Delta d}{d}\right| \tan\theta + \frac{0.9\lambda}{t\cos\theta}$. Multiplying by $\cos\theta$ and dividing by λ gives:

not a dangling participle, rather a correctly used gerund

$n\lambda = 2d\sin\theta$

$d = \frac{n\lambda}{2}\frac{1}{\sin\theta}$

$\frac{dd}{d\theta} = -\frac{n\lambda}{2}\frac{\cos\theta}{\sin^2\theta}$

$\frac{\Delta d}{\Delta\theta} = -d\frac{\cos\theta}{\sin\theta}$

$\rightarrow \Delta\theta\cos\theta = -\frac{\Delta d}{d}\sin\theta$

$\frac{\Delta\theta \cos\theta}{\lambda} = \left|\frac{\Delta d}{d}\right| \sin\theta + \frac{0.9}{t}$. By plotting $\frac{\Delta\theta \cos\theta}{\lambda}$ vs. $\frac{\sin\theta}{\lambda}$ the strain in the film and the thickness of the film is revealed.

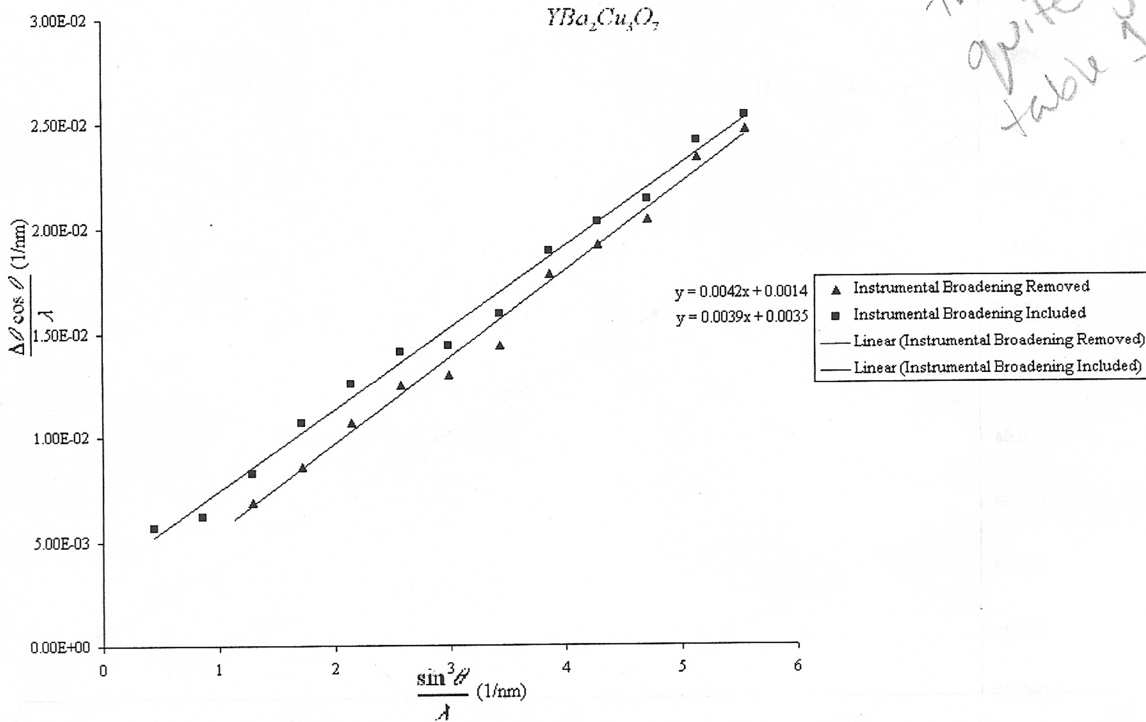

Figure 9 A plot revealing the strain and thickness of the YBCO film with and without the inclusion of the instrumental broadening.

Figure 9 details plots of the data with the instrumental broadening removed and included. Instrumental broadening only accounts for 0.03% of the strain, but its effect on the thickness is considerable.

Using the same analysis for determination of the lattice parameters, both the CeO_2 and Al_2O_3 films were calculated. Two peaks were observed for the ceria film and three peaks were observed for the sapphire as expected for highly oriented films with small

$$\frac{\Delta\theta \cos\theta}{\lambda} = \left|\frac{\Delta d}{d}\right| ...$$

thickness of the ...

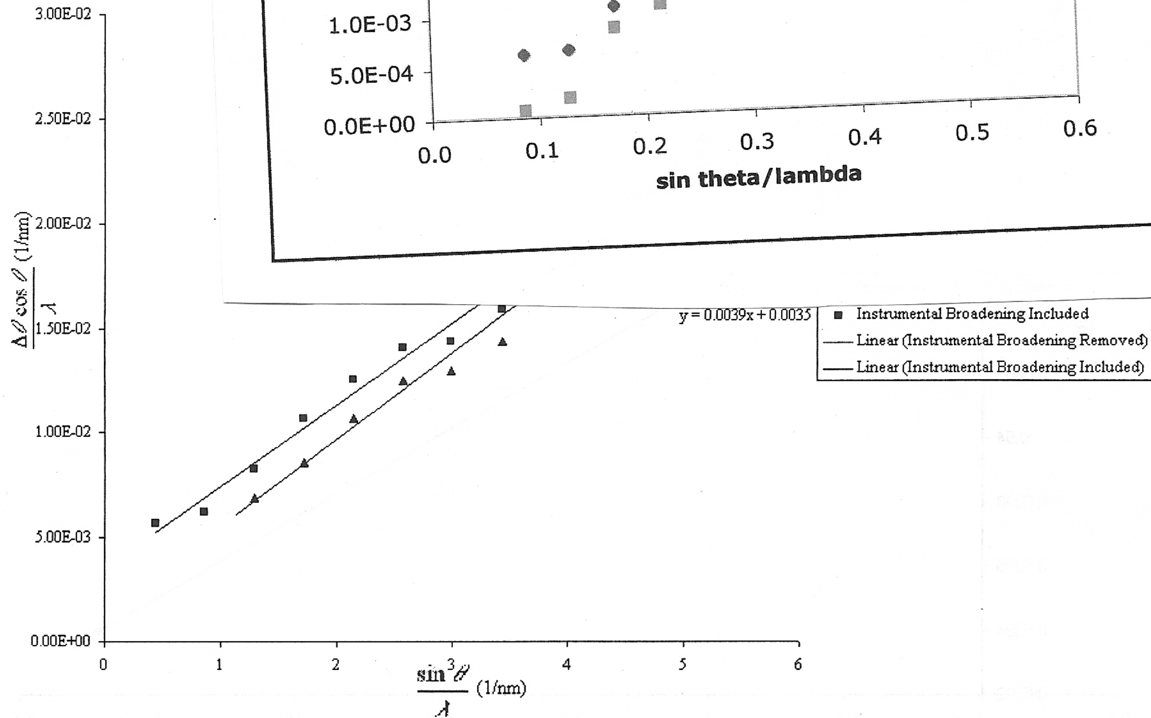

Figure 9 A plot revealing the strain and thickness of the YBCO film with and without the inclusion of the instrumental broadening.

Figure 9 details plots of the data with the instrumental broadening removed and included. Instrumental broadening only accounts for 0.03% of the strain, but its effect on the thickness is considerable.

Using the same analysis for determination of the lattice parameters, both the CeO_2 and Al_2O_3 films were calculated. Two peaks were observed for the ceria film and three peaks were observed for the sapphire as expected for highly oriented films with small

lattice parameters. Though there is a lack of data for these two films, analysis of this lattice parameter can still be performed with some confidence because the analysis on the $YBa_2Cu_3O_7$ film produced values within the expected range. Figures 10 and 11 detail the extrapolated values for CeO_2 and Al_2O_3 films respectively.

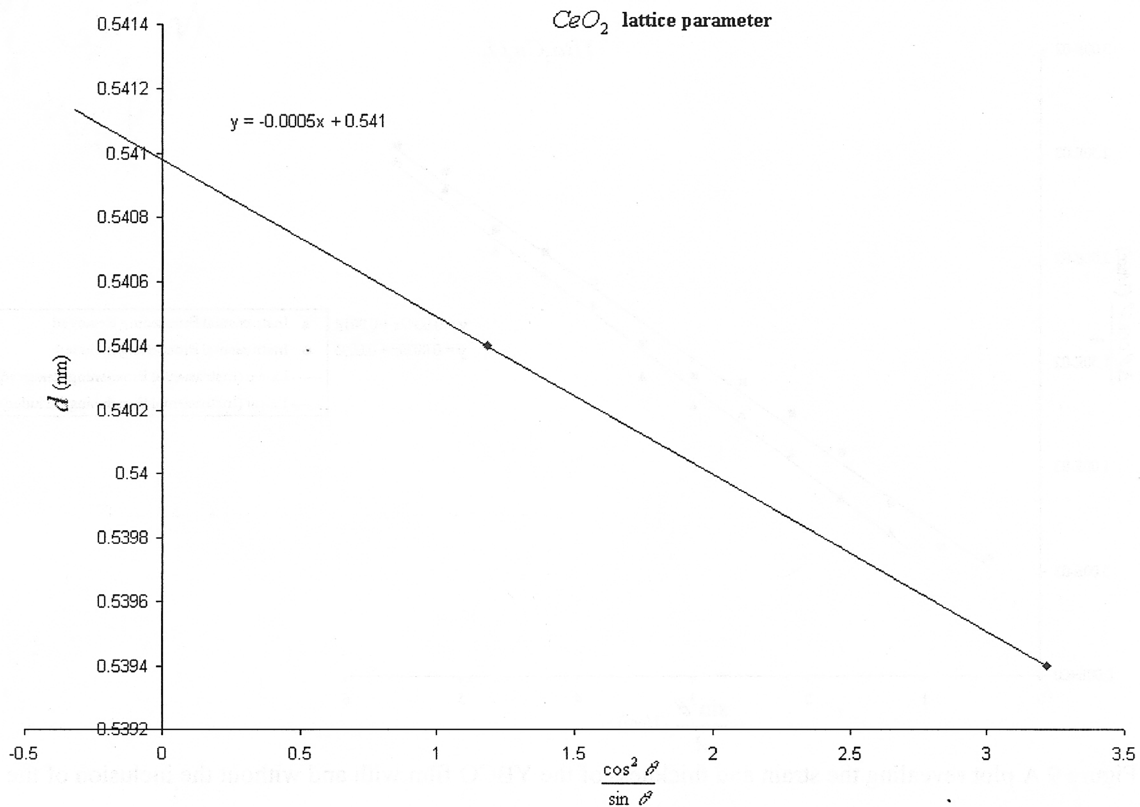

Figure 10 A regression plot of the ceria lattice constant. An extrapolated value of 0.541 nm was determined.

The value extrapolated for the cerium oxide film is 0.541 nm with an error of ± 0.001. This value agrees with the JCPDS value of 0.541nm (JCPDS 34-394).

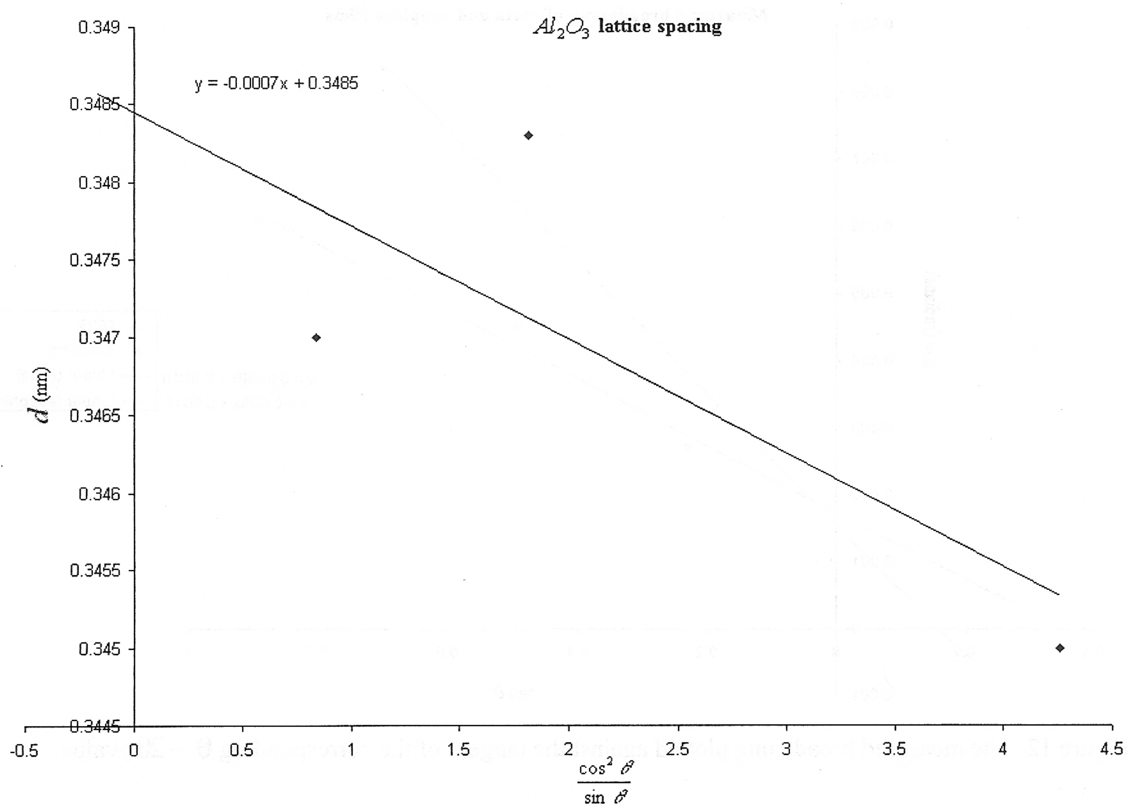

Figure 11 A regression plot of the sapphire lattice spacing as detected by the x-ray diffraction machine.

Above, the extrapolated value of sapphire lattice spacing is 0.3485nm with an error of ± 0.0015. It is important to remember that the lattice parameter above is what the XRD machine is detecting. In this instance, the lattice spacing is not a lattice constant for the film.

Below, Figure 12 shows a plot of the measured broadening in the ceria and sapphire films vs. $\tan\theta$. This plot shows that the strain in the sapphire film is larger than in the YBCO film. One would expect the strain in the substrate to be smaller than in the other films because of its larger thickness.

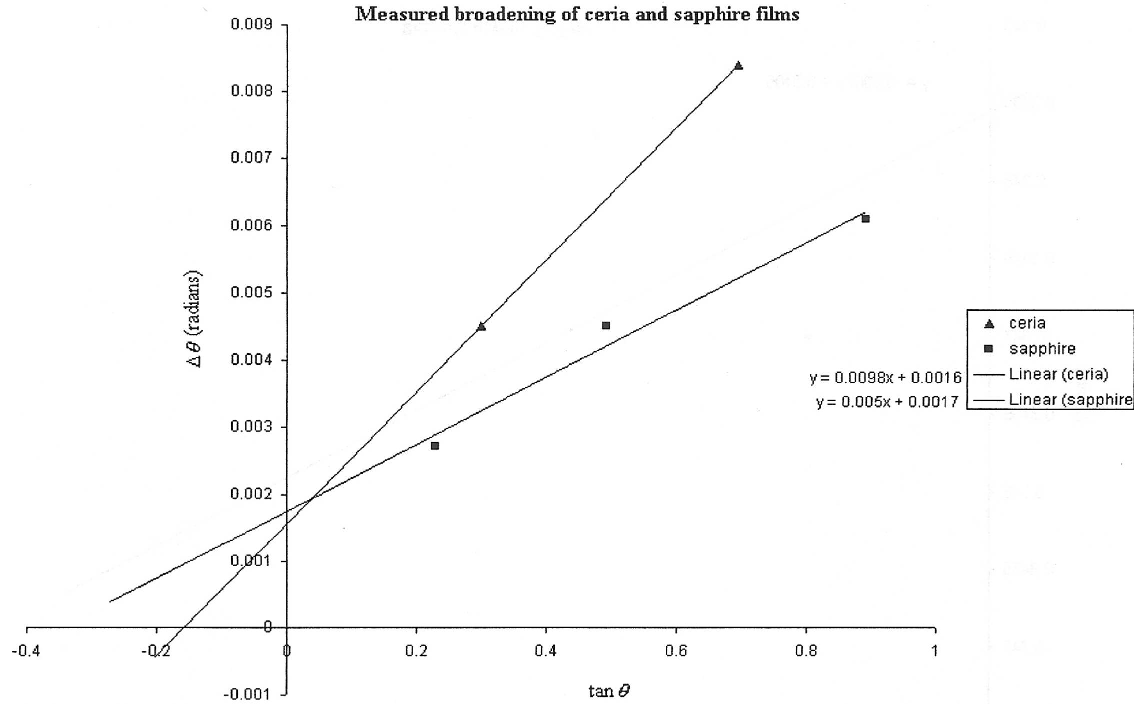

Figure 12 The measured broadening plotted against the tangent of the corresponding $\theta - 2\theta$ value.

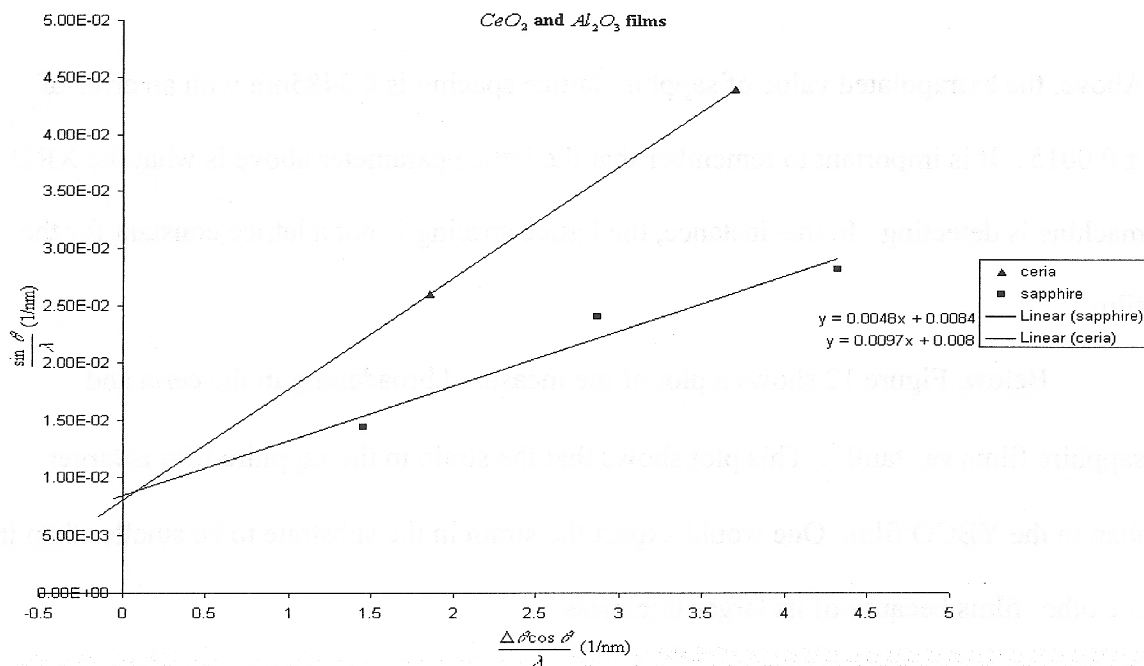

Figure 13 A plot of the broadening of the XRD peaks of the two films with the instrumental broadening removed.

	$\frac{\Delta d}{d}$	$\frac{\Delta d}{d}$ with removal of instrumental broadening	Thickness of film	Thickness of film with removal of instrumental broadening
$YBa_2Cu_3O_7$	0.44%	0.39%	257nm	642nm
CeO_2	0.98%	0.97%	81nm	112nm
Al_2O_3	0.5%	0.48%	75nm	107nm

Table 4 Comparison of strain and thickness for each film

Removing the effects of instrumental broadening does not change the strain in the buffer layer or substrate significantly. Figure 13 again shows that removal of instrumental broadening greatly changes the expected thickness of the films. This analysis leads to a conclusion that the sapphire data is not as reliable as it should be. As mentioned earlier, x-ray diffraction data should show a much stronger signal for the substrate than for the other films because it contains so much axis orientation in the film. When the peaks for the substrate are weak, it is possible that the sample was not properly mounted in the device (Dumkow, 1997). In some instances, degradation of substrate peaks due to unknown causes has been observed. Analysis of the strain in the sapphire film should reveal little if any strain in the crystal because it is so thick compared to the films. Yet, figure 13 shows that the strain of the substrate is on the order of the strain in the other films as well as the thickness being smaller than the YBCO film. This is further evidence that the sapphire data is unreliable.

Conclusion

Determination of the lattice spacing for all three films provided values that agreed with other literature, as expected. According to Dumkow, fully oxygenated YBCO films typically have a c-axis parameter that varies between 1.17 nm and 1.172 nm. The experimental analysis in this thesis agrees with these values. The values for the lattice spacing of the ceria and sapphire films are also in agreement with the JCPDF files.

Consideration of instrumental broadening in the strain of a film does not appear to be an overall importance. Removal of instrumental broadening changed the results by 0.03% in the strain of the YBCO film, while practically no change in the strain of the buffer layer or sapphire substrate films occurred. Expected thickness of the two top films was on the order of 200 nm. Figure 9 shows that for the YBCO film, removal of the instrumental broadening yields a thickness on the order of 650 nm while the original analysis yields a thickness on the order of 250 nm, which agrees with our expectation. The thickness of the ceria film using the latter analysis revealed a thickness of 112 nm. Also, one would expect the thickness of the substrate to be much larger than the top films. Figure 13 details that the thickness of the substrate is in fact smaller than the other two films. This is further evidence that the sapphire data is unreliable. The question of the true thickness of these films can be answered by using other spectroscopic methods such as TEM. These observations and analyses lead to further questions such as, at what thickness is it important to consider broadening due to instrument resolution? Further investigation of this sample is needed to fully understand the physical parameters of the system, but this thesis has shown the utility and importance x-ray diffraction can have when analyzing thin-film samples as well as crystals.

acknowledgements – Irene Dumkow
made films + took spectra

Bibliography

Cullity, B.D. (1978). Elements in x-ray diffraction(2nd ed.). Reading, MA: Addison-Wesley Publishing.

Dumkow, I. (1997). Oxygen-deficient YBCO films investigated by perturbed angular correlation spectroscopy. Ph.D. Thesis in Physics. Oregon State University. Corvallis, OR.

Hecht, E. (1987). Optics(2nd ed.). Reading, MA: Addison-Wesley Publishing.

Lide, D.R., ed. (1993). CRC Handbook of Chemistry and Physics(73rd ed.). Boca Raton. CRC Press.

Ohring, M. (1992). The material science of thin films. San Diego, CA: Academic Press.

Prakash, S., Bunshah, R.F. (1992). Crystallinity of $Y_1Ba_2Cu_3O_{7-x}$ films grown on MgO by activated reactive evaporation. Journal of material research, 7(9), 2343-2348.

TA 401. J6671

Maul, M., Schulte, B., Haussler, P., Adrian, H. (1994). $Y_1Ba_2Cu_3O_{7-x}$ thin films on Sapphire with buffer layers of CeO_2. Physica B. 2285-2286.

QC1.P4153

Merchant, P., Jacowitz, R.D., Tibbs, K. Taber, R.C., Laderman, S.S. (1991). Surface resistance of epitaxial $Y_1Ba_2Cu_3O_7$ thin films on CeO_2 diffusion barriers on Sapphire. Applied physics letters, 60(6). 763-765.